

# Preliminary analysis of vertical profiles of polarimetric radar observables in complex orography for operational purpose.

Mario Montopoli<sup>1,2</sup>, Gianfranco Vulpiani<sup>3</sup>

<sup>1</sup>Dep. of Information Engineering, Electronics and Telecommunications, Sapienza University of Rome, Rome, Italy

<sup>2</sup>CETEMPS, University of L'Aquila, Via Vetoio, 67100, L'Aquila, Italy

<sup>3</sup>Department of Civil Protection, Rome, Italy



Mario Montopoli

(Dated: 16 July 2014)

## 1 Introduction

The vertical variations of the radar variables are largely studied in radar meteorology for the identification of the predominant shape of the precipitation profiles. Such identified profiles, usually categorized for convective and stratiform rain regimes, are used to project radar observations, available at given altitudes, to levels close to the ground. Radar derived rain estimates that make use of the projections of the radar variables involved in the rain estimation close to the surface, are expected to be more consistent with ground reference, usually rain gauge or disdrometers. Thus, the identification of vertical profiles has an important role in the radar quantitative precipitation estimation (QPE) especially in those areas that show complex orography and where, as a consequence, the radar installations are positioned at high altitudes to avoid clutter contamination. In those situations, there is an additional complexity represented by the partial identification of the observed vertical profiles which might results incomplete and limited to the higher portion of the atmosphere, thus making the QPE very challenging. The radar quantities that show a well-defined vertical structures are the co-polar reflectivity ( $Z_{HH}$ ), the cross polar correlation coefficient ( $\rho_{HV}$ ) and the radial doppler velocity ( $V_R$ ) even though  $\rho_{HV}$  and  $V_R$  are mainly used for identifying melting layer boundaries whereas  $Z_{HH}$  is actually used for QPE.

Independently from the radar variable analyzed, the definition the vertical profiles (VPs) usually follows some typical steps: i) identification of homogeneous areas in terms of precipitation regimes, ii) calculation of the apparent profile or some of its apparent features, iii) compensation for the antenna convolution effects to obtain the “true” vertical profile, iv) application of the identified profile to project observations at the ground level. The terms “apparent” is used to define a quantity as it is measured by the radar, i.e.: the result of the convolution between the radar antenna radiation diagram and the true unknown quantity. On the contrary, the term “identified” is often used in the reference literature to indicate an estimate of the deconvolved profile.

The methods so far proposed in literature for the calculation of the VPs can be grouped into five categories. They are: *i) direct estimates* (Germann and Joss 2002) where apparent profiles are calculated from radar volumes for range distances less than approximately 60 km without any particular treatment for reducing the smoothing effects due to the antenna convolution; *ii) indirect estimates* (Marzano et al., 2004) where apparent quantities at lower altitudes (i.e. not sampled by the radar) are estimated using information available at higher altitudes. The connection between quantities at higher and lower altitudes is implemented training neural networks or multiple regression polynomials; *iii) shape synthesis* (Kitchen et al. 1994; Tabary 2007, Vignal et al. 1999): where parametric models are used to describe, or fit, the apparent or the identified profiles. Thus, the radar variables are used to estimate the parameters of the VP models rather than directly the VPs. In case of missing portions of the VPs, some simplifying assumptions have to be done to produce a complete profile; *iv) numerical identification* (Andrieu and Creutin 1995; Vignal et al. 1999; Borga et al. 2000; Kirstetter et al. 2010.) where the ratio of horizontal profiles of reflectivity  $F_Z = Z(r, \theta_i) / Z(r, \theta_j)$ , between two antenna elevations ( $\theta_i$  and  $\theta_j$ ) is used as a proxy for the estimation of the identified vertical profile of  $Z_{HH}$ . The procedure is then aimed at finding a synthetic VP of  $Z_{HH}$ , which is mostly consistent with  $F_Z$  through a minimization process; *v) physical models*: (Kirstetter et al. 2013) where forward models of vertical profiles are used to generate a dataset of synthetic possible vertical profiles for the observed scene. The most representative VP of the observed scene is then found minimizing a measure of the difference between the observed profile and the set of possible synthetic profiles.

In this work a preliminary study of the methods of extraction of VPs is carried out. Polar Coordinates VPs Extraction (PCE) and Cartesian Coordinates VPs extraction (CCE) methods are explained and compared each other. VPs of  $Z_{HH}$  and  $\rho_{HV}$  are extracted and their features are discussed for several case studies in the view of their use in an operational context for improving QPE. Cases of incomplete VPs are shown as well and possible strategies to tackle these particular cases are analyzed. Radar volumes from the Mt. Pettinascura, (Cosenza, Italy) operational C-Band radar are used for the aforementioned purpose. Pettinascura radar is part of the national network managed by the Department of Civil Protection (DPC). Since most of the Italian radar sites are in a complex orography environment, this study is preparatory for developing custom solutions for the compensation of vertical variability effects for the DPC radars in Italy.

The work is organized in four sections. Section 2 describes the framework of the vertical profile correction giving explanations of the methods used to extract profiles from radar volumes. Section 3, describes the processing chain used to elaborate the radar data before extracting the vertical profiles. Section 4 gives some details on the case studies analyzed and of the radar features. The work closes with section 5 where result's discussion is given.

## 2 Strategies for extracting vertical profiles from radar polar volumes

In this section two methods for the VP calculation from radar volumes, or a portion of it, are described. The two methods are the Polar Coordinates VPs Extraction (PCE) and Cartesian Coordinates VPs extraction (CCE) methods.

However, VPs extracted by these methods, when used for surface rain retrieval, comply with some common assumptions here recalled. The treatment that follows is described in terms of  $Z_{HH}$ . Usually, the true unknown profile of reflectivity ( $Z_t$ ) (i.e. deconvolved profile) is seen as the results of the product of two components:  $Z_t(\mathbf{u},0)$  and  $Z_m(h)$ . The former are the true values closest to the ground ( $h \approx 0$ ) at positions  $\mathbf{u}=(x,y)$ , while the latter is the normalized true profile which describe the vertical variations for each altitude ( $h$ ). Thus it holds:

$$Z_t(\mathbf{u},h) = Z_t(\mathbf{u},0) \cdot Z_m(h) \quad (1)$$

Eq. (1) says that  $Z_m$  is the same in each position  $\mathbf{u}$  or, in other words, the normalized vertical profile is spatially invariant. As far as  $Z_t(\mathbf{u},0)$  is homogeneous over the spatial domain of analysis ( $D_s$ ), such as for example happens during well stratified rain events, we can assume that:

$$\langle Z_t(\mathbf{u},0) \rangle_{D_s} = Z_t(0) = Const. \quad (2)$$

and, (1) leads to:

$$Z_t(\mathbf{u},h) = Z_t(0) \cdot Z_m(h) \quad (3)$$

The goal of any procedure for VP compensation is the calculation of the term  $Z_m(h)$ . Unfortunately, due to finite antenna aperture, the radar measures an apparent reflectivity ( $Z_a$ ), which is the convolution of the true reflectivity and the antenna gain ( $G$ ) within each sampling volume:

$$Z_a(\mathbf{u},h) = \int_{u_{min}}^{u_{max}} \int_{h_{min}}^{h_{max}} Z_t(s,h) \cdot G(s,h) ds dh = Z_t(0) \cdot Z_{an}(h) \quad (4)$$

where  $h_{max}$ ,  $h_{min}$ ,  $u_{min}$  and  $u_{max}$  are the vertical and horizontal coordinates of the boundaries of a given sampling volume and where we used (3) to derive the third term of (4). The quantity  $Z_{an}$  in (4) is:

$$Z_{an}(h) = \int_{u_{min}}^{u_{max}} \int_{h_{min}}^{h_{max}} Z_m(s,h) \cdot G(s,h) ds dh \quad (5)$$

In terms of dB, equation (4) can be rewritten as:

$$Z_t dB(0) = Z_a dB(\mathbf{u},h) - Z_{an} dB(h) \quad (6)$$

From (5) the true value close to the ground is obtained from the difference, at a given altitude ( $h$ ) and in each position  $\mathbf{u}$ , between the apparent measured reflectivity and the normalized apparent profile, which is a pre-defined profile. However, (6) is valid only when (2) is true. This implies that in (6),  $\mathbf{u}$  varies within  $D_s$  and  $D_s$  must only include regions where  $Z_t(\mathbf{u},0)$  is homogeneous as much as possible. Thus,  $D_s$  have to be identified before applying a successful procedure of vertical profile compensation. As a consequence,  $Z_{an}$  have to be spatial invariant in the domains  $D_s$  and for this reason it is usually the result of a spatial average in the domain  $D_s$ . The choice of  $D_s$  can be very critical because from this choice depends the representativeness of  $Z_{an}$  in (6).

### 2.1 Cartesian Coordinates vertical profile extraction (CCE).

This method (figure 1, right panel) extract profiles along vertical directions for each position  $\mathbf{u}=(x,y)$ . To do that a polar to Cartesian coordinate conversion is applied before proceeding to extract the vertical profiles eq.(7). The advantage of this methodology is the ability to extract a profile for each position  $\mathbf{u}$  that can be grouped subsequently as needed, eq. (8) in the domain  $D_s$  in (9). The drawback is the method's dependency from the resampling procedure which sampling intervals are subjectively chosen by the user. In formulas the CCE method is as follows:

$$Z_a(x, y, h) \leftarrow Z_a(r, \theta, \varphi) \quad (7)$$

$$Z_{an}(h) = \frac{\langle Z_a(\mathbf{u}, h) \rangle_{D_s}}{\langle Z_a(\mathbf{u}, 0) \rangle_{D_s}} \quad (8)$$

$$D_s = \{(x, y) \mid x \in [x_{\min}, x_{\max}] \& y \in [y_{\min}, y_{\max}]\} \quad (9)$$

Note, in (8) the symbol “ $\langle \bullet \rangle$ ” is an average in  $x$  and  $y$  directions.

## 2.2 Polar Coordinates vertical profile Extraction (PCE)

This method (figure 1 left panel) is based on the assumption that the radial variations of the analyzed quantity, is dominated from its vertical gradient. Under this assumption each radar ray, at a fixed elevation and azimuth, gives some information on the vertical profile. In this case the normalized apparent reflectivity is calculated directly in polar coordinates ( $r$ =range,  $\varphi$ =azimuth,  $\theta$ =elevations) thus preserving the original scan geometry:

$$Z_{an}(h) = \frac{\langle Z_a(r, \theta, \varphi) \rangle_{D_s}}{\langle Z_a(0) \rangle_{D_s}} = \frac{Z_a(r, \theta)}{\langle Z_a(0) \rangle_{D_s}} = \frac{Z_a(h)}{\langle Z_a(0) \rangle_{D_s}} \quad (10)$$

In (10), “ $\langle \bullet \rangle$ ” is an average along the azimuth directions and the domain  $D_s$  is as follows:

$$D_s = \{(r, \varphi) \mid r \in [r_{\min}, r_{\max}] \& \varphi \in [\varphi_{\min}, \varphi_{\max}]\} \quad (11)$$

The dependency between  $Z_a(r, \theta)$  and  $Z_a(h)$  in (10) is through the expression of radar beam height with respect the radar antenna altitude in the standard atmosphere:

$$h = f(r, \theta) = \left[ r^2 + ae^2 + 2ae \cdot r \cdot \sin(\theta) \right]^{0.5} - ae \quad (12)$$

where  $ae=4/3 \cdot 6371$  and  $h$  is in [km]. It should be noted that due to the nonlinear relation between  $h$ ,  $r$  and  $\theta$ , the profiles obtained using (10), are extracted at irregular altitudes. Additionally, the profiles extracted at higher elevations undergo a smaller effect of the antenna convolution in the vertical direction. For these two reasons, when the PCE method is used for the calculation of VPs, it is important to introduce further elaborations to homogenize the profiles obtained at the various elevations and average them in a proper way. In this work we firstly interpolated the elevation-dependent profiles to a common vertical reference grid with spacing  $\Delta h=0.5$  km and then we performed a weighted average of all elevation-dependent profiles weighting less the profiles extracted at low elevations where residual ground clutter likely corrupt the VPs and where the convolution effects are more evident. **Figure 2** shows an example of the VPs extracted for each available elevation of Mt. Pettinascura radar, (Italy) for  $Z_{HH}$  and  $\rho_{HV}$  and the resulting profile after the weighted average.

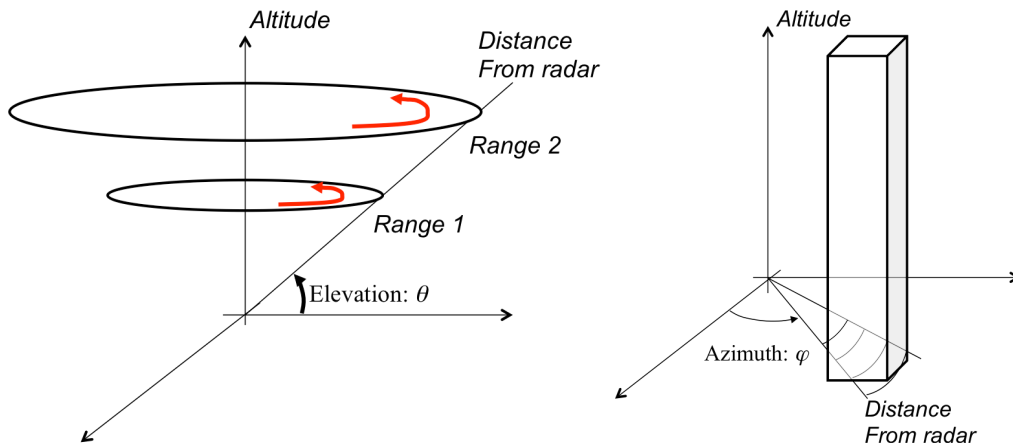


**Figure 1:** Schemes for the calculation of vertical profiles. Left: *Polar Coordinates vertical profile Extraction (PCE)*. Right: *Cartesian Coordinates vertical profile extraction (CCE)*.

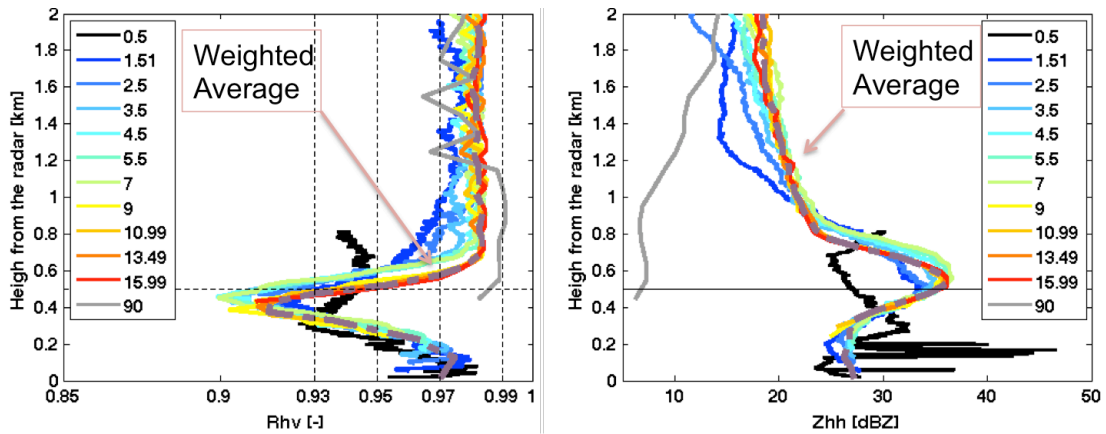


**Figure 2:** Vertical profiles (VPs) of  $\rho_{HV}$  (left) and  $Z_{HH}$  (right) extracted on Dec. 1<sup>st</sup>, 2013 at 00:00 UTC using Polar Coordinates vertical profile Extraction (PCE). Panel's legend indicates elevations [deg] for which VPs are extracted. The result weighted average profile is shown as dashed line in each panel.

### 3 Radar data processing

Pettinascura radar volumes are processed using techniques already consolidated in literature. Partial beam blocking (PBB) is compensated using the approach of Bech et al., 2003 where the PPB map is obtained from digital terrain model. Ground clutter is filtered out applying a threshold on the quality map (Q). Q is generated following the methodology suggested in Vulpiani et al., 2012 and it is obtained weighting, with given membership functions, the clutter map, the textures of  $Z_{DR}$ ,  $\rho_{HV}$  and filtered differential phase shift ( $\phi_{DP}$ ). The clutter map is derived from long sequence of clear air scans. Filtered  $\phi_{DP}$  and the specific differential phase  $K_{DP}$  are obtained applying the procedure from Vulpiani et al. (2012). The phase filtering method is iterative and it automatically removes spikes, offset and wrapped values in  $\phi_{DP}$ . No automatic procedure for the calibration of  $Z_{DR}$  are actually implemented even though we verified *a posteriori* the excellent  $Z_{DR}$  accuracy, within 0.1 dB, using vertical scans. However, the latter quantity is not used in this analysis.

### 4 Case studies

Four case studies are selected to preliminarily discuss the characteristic of vertical profiles as seen by the Pettinascura radar (**figure 3** left panel). Pettinascura radar is part of the Italian radar network and it is managed by the Italian department of civil protection that is in charge for its maintenance and its rain products. The Pettinascura radar is positioned at lon/lat/height=[16.6183, 39.3698, 1.725] in decimal deg, decimal deg and km, respectively. The radar variables available from the Pettinascura radar are the co-polar reflectivity, differential reflectivity, cross polar correlation coefficient, specific differential phase and the radial velocity:  $Z_{HH}$ ,  $Z_{DR}$ ,  $\rho_{HV}$ ,  $K_{dp}$ ,  $V_r$ , respectively. However, in this preliminarily analysis only  $Z_{HH}$  and  $\rho_{HV}$  are used.

The selected case studies are Dec. 1<sup>st</sup>, 2014, Feb. 1<sup>st</sup>, 2014, Feb. 4<sup>th</sup> 2014 and Feb. 12<sup>nd</sup>, 2014. These cases are interesting because, as evidenced later on, the Pettinascura radar often lies within or slightly above the bright band level. This situation causes large underestimation of rain accumulations at far distances from the radar thus vanishing any quantitative analysis by the meteorologist. Figure 3 (right panel) shows an example of the selected cases on Dec. 1<sup>st</sup>, 2014 at instants 00:00 00:20 and 00:55 UTC. All case studies have been acquired in polar coordinates by the Pettinascura radar with range, azimuth and time sampling of 0.15 km, 1 deg and 5 min, respectively. Seldom, could happen that some polar volumes are missing and the time sampling degrades to 10 min. Twelve elevations are available [deg]. They are at 0.5, 1.51, 2.5, 3.5, 4.5, 5.5, 7, 9, 10.99, 13.49, 15.99 and 90 deg. The 90 deg elevation is not used in the analysis for two reasons. Firstly, the high altitude of the radar limit the utility of the vertical scans which would produce incomplete profiles. Secondly due to some hardware issues of the TLR limiter, the first few gates are of poor quality and for this reason they are discarded from the analysis. Unfortunately, even few gates are essential for vertical profiles obtained by vertical scans.

### 5 Discussions

The vertical profiles of  $Z_{HH}$ ,  $\rho_{HV}$ , hereafter, respectively,  $VP_{Z_{HH}}$  and  $VP_{\rho_{HV}}$  are extracted, using PCE method, for each volume (i.e.  $D_S$ =whole volume) at each instant of each of the four cases selected. However, thresholds on  $Z_{HH}$  and  $\rho_{HV}$  are set so that values less or equal to 5 dB and 0.8 are discarded from the analysis, respectively. Difference in the PCE and CCE methods of VP extraction are found to be not larger than 3 dB for  $VP_{Z_{HH}}$  (not shown). These differences are found especially in the presence of strong variations of  $Z_{HH}$ . However, in this analysis we prefer to use the PCE method since it preserves

more the polar geometry of the radar acquisitions. **Figure 3**, right panels, third and forth panel's row, gives an example of  $VPZ_{HH}$  and  $VP\rho_{HV}$  profiles. A first important guidance can be drawn by the temporal sequence of  $VP\rho_{HV}$  and  $VPZ_{HH}$  in this figure. While  $VP\rho_{HV}$  is quite steady within the hour represented in figure 3,  $VPZ_{HH}$  shows marked difference above the melting layer, at higher altitudes in the iced part. In particular at 00:00 UTC we have a  $VPZ_{HH}$  that decreases at a rate of approximately  $-7\text{ dB/km}$  as in Fabry et al., 1995. Just after 55 min  $VPZ_{HH}$  modifies its shape in the ice part and its rate of decrease is nearly zero. This indicates that to avoid large errors in the compensation of VP we have to consider sub-hourly variations. This can be achieved, for example, by implementing an adapting scheme that update the VP at each radar scan, taking into account the past extracted VPs, to mimic the VP variations at each radar time step (Germann et al., 2002). **Figure 4** shows a zoomed version of the profiles in figure 3 in the third and forth row left panels. From this figure it appears evident the mismatch between the altitudes where  $Z_{HH}$  is maximum and  $\rho_{HV}$  is minimum. From both profiles the thickness of the bright band results to be approximately 500 m. Matrosov et al. in 2007 already noted this aspect and he explained it as a different behavior of  $\rho_{HV}$  and  $Z_{HH}$  within the melting layer. Basically, the altitude where snow starts melting and, as a consequence  $Z_{HH}$  reaches its maximum, does not coincide with the altitude for which the number of snow and ice particles coexists, or in other words when  $\rho_{HV}$  reaches its minima. Thus it is important to take into account the mismatch between  $VPZ_{HH}$  and  $VP\rho_{HV}$  whenever, for example,  $VP\rho_{HV}$  is used to define the BB layer and to constrain the parameters of a model of  $VPZ_{HH}$ . In our example of figure 4, the mismatch between  $VPZ_{HH}$  and  $VP\rho_{HV}$  is of the order of 150 m that leads to difference up to 9 dB in the BB where strong variations of  $Z_{HH}$  with the height of the order of 60 dB/km occurs.

The last analysis is in **figure 5**, where the occurrences of  $VPZ_{HH}$  and  $VP\rho_{HV}$  are color-coded in the upper and lower panels, for each event, respectively. From this figure we note as the 0°C isotherms (red dotted lines), derived by the radiosondes launched from Brindisi at 00, 12 of each day matches very well with the points where  $\rho_{HV}$  starts decreasing from its nearly constant value in the ice layer. This fact confirms the usefulness of  $\rho_{HV}$  in the freezing level identification. On the other hand, the histograms of  $VPZ_{HH}$  show a very high variability, especially the slope of the ice part is far to be constant. This suggests that approaches that use climatological  $VPZ_{HH}$  may lead to large errors in the reconstructed rain fields at the ground level. Eventually, for the case of February 1<sup>st</sup>, 2014 the slope of  $VPZ_{HH}$ , around altitudes of 4 km, seems to have a marked increase. This might suggest the use of an additional slope parameter to describe the  $VPZ_{HH}$  by linear models.

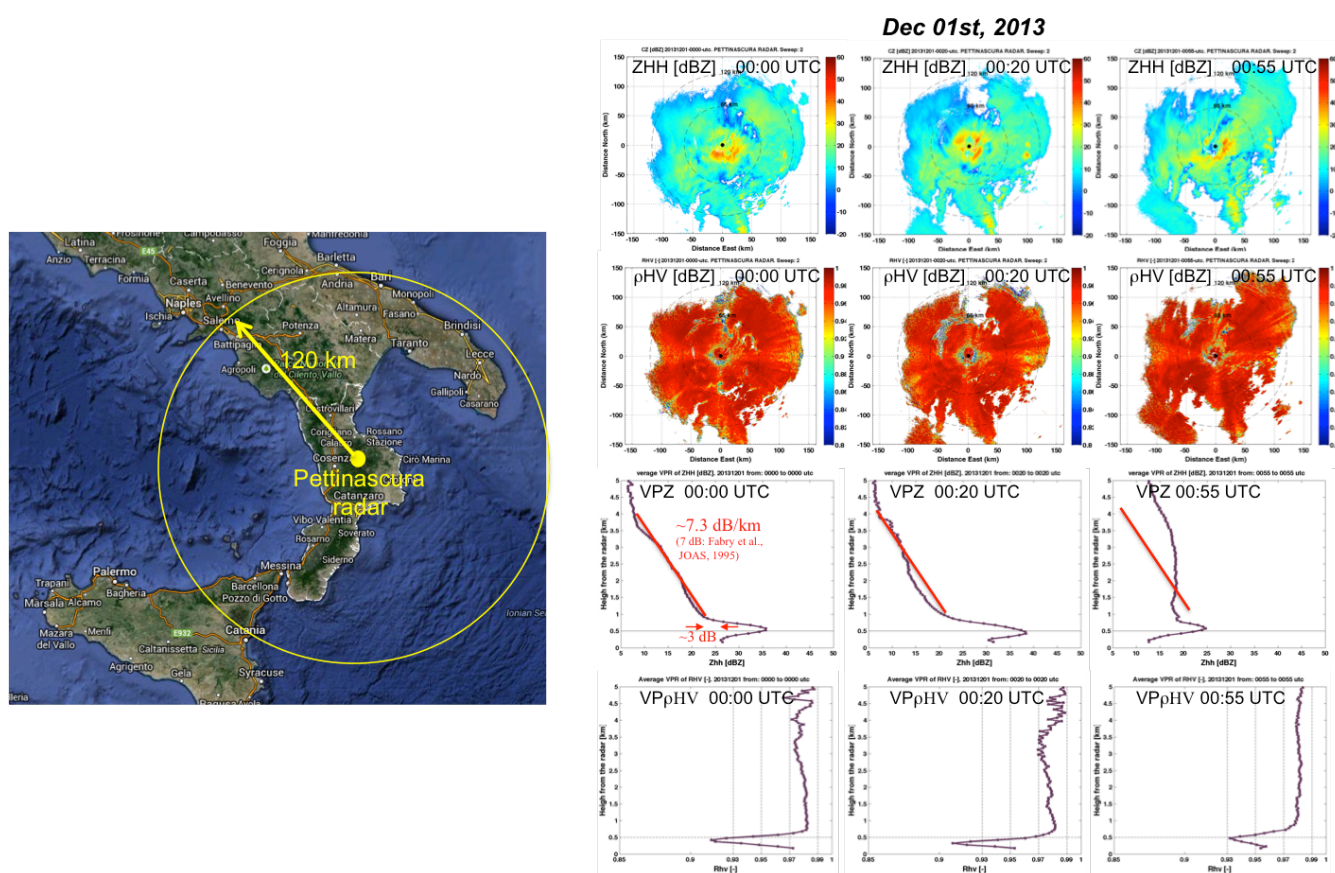


**Figure 3:** Left panel. Pettinascura radar located at lon/lat=[16.6183, 39.3698] with its coverage up to 200 km. Right: PPI of  $Z_{HH}$  (first row of panels),  $\rho_{HV}$  (second row of panels) at elevation of 1.51 deg,  $VPZ_{HH}$  (third row) and  $VP\rho_{HV}$  (fourth row) at instant, from left to right, 00:00, 00:20 and 00:55 UTC on Dec, 1<sup>st</sup>, 2013.



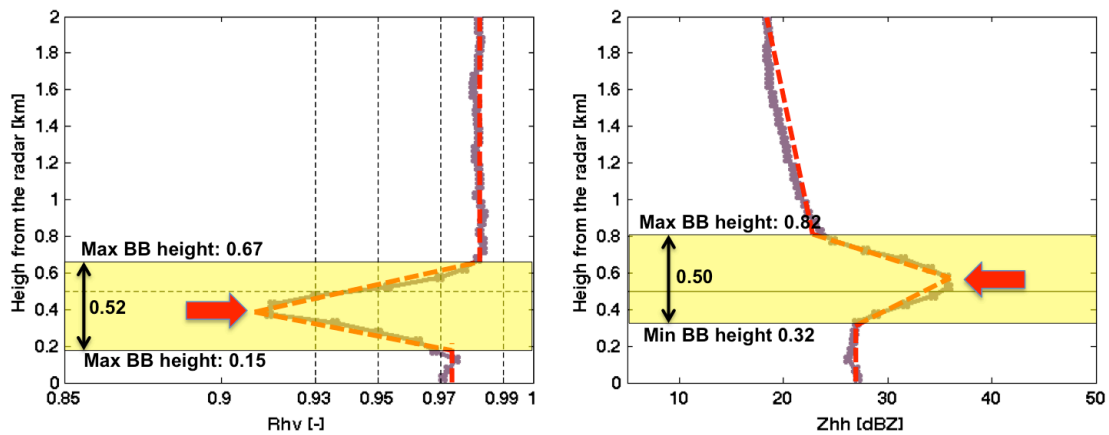


**Figure 4:** Vertical profile of  $\rho_{HV}$  (left) and  $Z_{HH}$  (right) for Dec. 1<sup>st</sup>, 2013 at 00:00 UTC (brown solid line). The y-axis is limited to 0-2 km to better appreciate variations. Red dotted lines shows an hypothetical VP linear model.

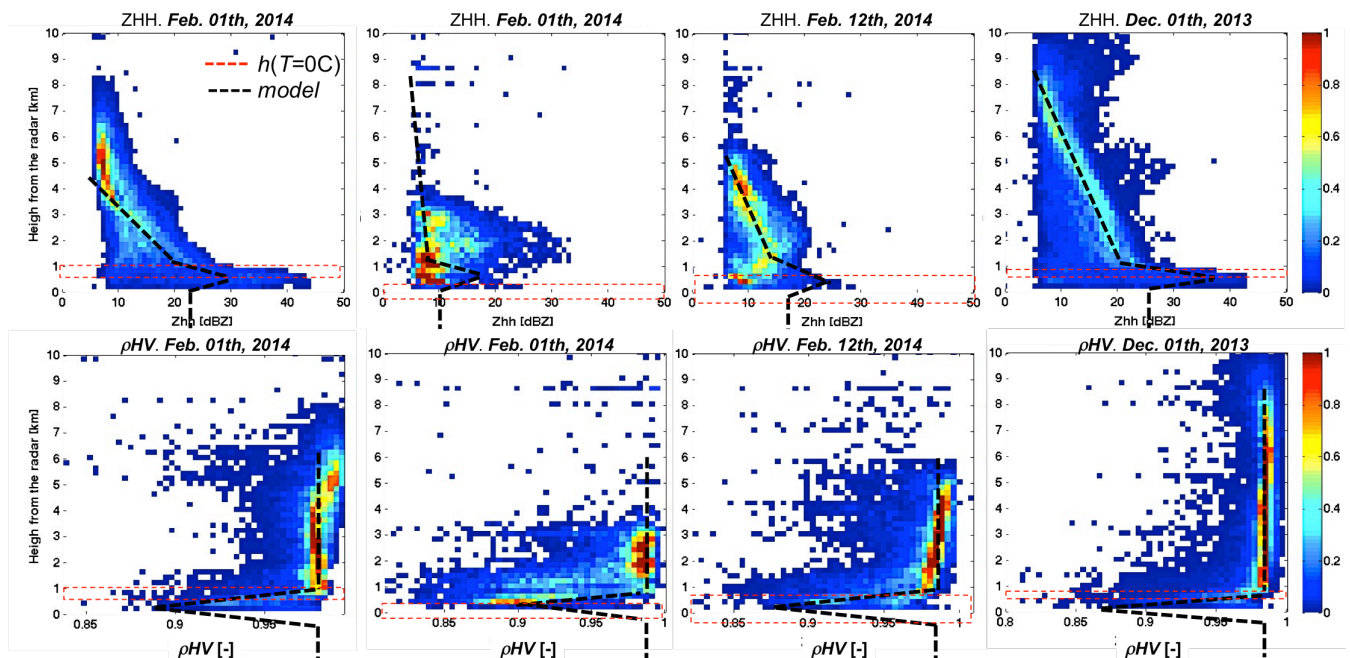


**Figure 5:** bi-dimensional histograms of vertical profiles as a function of heights from the radar (positioned at 1.725 km) for each event as indicated in the title of each panel. Upper rows profiles of  $Z_{HH}$ . Lower panels: profiles of  $\rho_{HV}$ . Black dashed lines are linear models qualitatively fitted for each histogram. Colours refer to occurrences [%]. Red bars indicates the heights at 0 C isotherm as derived by the 2 daily radiosondes launched from Brindisi (Italy).

## 6 Acknowledgements

A special thank is due to Dr. S. Meroi and P. Pagliara of the Italian Dept. of Civil Protection (Italy) through the “LabRadMet” agreement with the University of Rome La Sapienza.

## 7 References

- Andrieu, H., and J. D. Creutin, 1995: Identification of vertical profiles of radar reflectivity using an inverse method. Part I: Formulation. *J. Appl. Meteor.*, 34, 225–239.
- Bech, J., B. Codina, J. Lorente, and D. Bebbington, 2003: The sensitivity of single polarization weather radar beam blockage correction to variability in the vertical refractivity gradient. *J. Atmos. Oceanic Technol.*, 20, 845–855.
- Borga, M., F. Tonelli, R. J. Moore, and H. Andrieu, 2000: Long- term assessment of bias adjustment in radar rainfall estimation. *Water Resour. Res.*, 38, 1226, doi:10.1029/2001WR000555.
- Fabry, F., and I. Zawadzki, 1995: Long-Term Radar Observations of the Melting Layer of Precipitation and Their Interpretation. *J. Atmos. Sci.*, 52, 838–851.

- Germann, U., and J. Joss, 2002: Mesobeta profiles to extrapolate radar precipitation measurements above the Alps to the ground level. *J. Appl. Meteor.*, 41, 542–557.
- Kirstetter, P. E., H. Andrieu, G. Delrieu, and B. Boudevillain, 2010: Identification of vertical profiles of reflectivity for correction of volumetric radar data using rainfall classification. *J. Appl. Meteor. Climatol.*, 49, 2167–2180.
- Kirstetter, Pierre-Emmanuel, Hervé Andrieu, Brice Boudevillain, Guy Delrieu, 2013: A Physically Based Identification of Vertical Profiles of Reflectivity from Volume Scan Radar Data. *J. Appl. Meteor. Climatol.*, 52, 1645–1663. doi: <http://dx.doi.org/10.1175/JAMC-D-12-0228.1>
- Kitchen, M., R. Brown, and A. G. Davies, 1994: Real-time correction of weather radar data for the effects of bright band, range and orographic growth in widespread precipitation. *Quart. J. Roy. Meteor. Soc.*, 120, 1231–1254.
- Marzano Frank Silvio, Senior Member, IEEE, Gianfranco Vulpiani, and Errico Picciotti, "Rain Field and Reflectivity Vertical Profile Reconstruction From C-Band Radar Volumetric Data", *IEEE TRANSACTIONS ON GEOSCIENCE AND REMOTE SENSING*, VOL. 42, NO. 5, MAY 2004 1033
- Matrosov, Sergey Y., Kurt A. Clark, David E. Kingsmill, 2007: A polarimetric radar approach to identify rain, melting-layer, and snow regions for applying corrections to vertical profiles of reflectivity. *J. Appl. Meteor. Climatol.*, 46, 154–166. doi: <http://dx.doi.org/10.1175/JAM2508.1>
- Tabary, P., 2007: The new French operational radar rainfall product. Part I: Methodology. *Wea. Forecasting*, 22, 393–408.
- Vignal, B., H. Andrieu, and J. D. Creutin, 1999: Identification of vertical profiles of reflectivity from voluminal radar data. *J. Appl. Meteor.*, 38, 1214–1228.
- Vulpiani, G., M. Montopoli, L. Delli Passeri, A. Gioia, P. Giordano, F.S. Marzano, 2012: On the Use of Dual-Polarized C-Band Radar for Operational Rainfall Retrieval in Mountainous Areas. *J. Appl. Meteor. Climatol.*, 51, 405–425.